

Effects of Electron and Proton Radiation on Perovskite Solar Cells for Space Solar Power Application

Jing-Shun Huang¹, Michael D. Kelzenberg¹, Pilar Espinet-González¹, Colin Mann², Don Walker², Ali Naqavi¹, Nina Vaidya¹, Emily Warmann¹, and Harry A. Atwater¹

¹California Institute of Technology, Pasadena, CA 91125, United States

²Aerospace Corporation, El Segundo, CA 90245, United States

ABSTRACT — We report the effects of high energy electron and proton radiation on perovskite solar cells. For irradiation with 1 MeV electrons, at fluence from 10^{12} to 10^{16} cm^{-2} , there are no significant changes in the morphology and the crystal phase in the perovskites, and the perovskite solar cells show only slight degradation in photovoltaic performance and spectral response. The results from Monte Carlo simulations show most of the electrons completely penetrate through all of the layers of solar cells with little scattering. In addition, 50 keV proton radiation with fluence of 10^{12} cm^{-2} has no significant impact on the open-circuit voltage or short-circuit current, and degrades only the fill factor. We have further found that the fill factor can be restored with a vacuum annealing process. The results suggest that perovskites have superior electron and proton radiation tolerance, and thus hold particular promise for space applications.

I. INTRODUCTION

Although crystalline Si solar modules dominate the photovoltaics market with an affordable price per watt and proven reliability, there are other needs for decentralized or mobile power generation for which other solar technologies are favorable. For example, space solar power, unmanned aerial vehicles (UAVs), and solar blimps require solar cells with high specific power (i.e., power to weight ratio). These applications require a combination of high photovoltaic performance, minimal weight, flexibility, mechanical resilience, working stability, long service life, and, ideally, low cost.

For space solar power applications, photovoltaic cells are subject to high-energy charged particle irradiation from space, which typically causes severe degradation of the cells' photovoltaic performance [1]. To prevent this, a thin layer of cover glass (typically up to hundreds of microns thick) is required to screen the solar cells from radiation, which inevitably increases the module weight and launch.

Today's mainstream solar technology for space applications, III-V compound solar cells, offers excellent efficiency approaching or exceeding 30% (AM0), and have a long heritage of reliability when adequately protected from radiation in space. However, other types of solar cells may prove superior for space applications if they are capable of achieving even higher specific power, or are intrinsically more radiation resistant, than established technologies, especially if they can be produced at lower cost.

Among various solar cell technologies, organo-lead halide perovskite solar cells have recently emerged as a potentially low-cost material capable of over 22% efficiency (AM1.5G). They have further shown a specific power of 26 W/g [2], a 20-fold increase over that of thin film silicon cells or thin film single-junction GaAs cells (up to 1.3 W/g) [3]. Although their extreme sensitivity to moisture has impeded their large-scale adoption for terrestrial applications, it is interesting to consider their use in space, where they would not be subject to atmospheric moisture after being launched. To our knowledge, their radiation hardness and suitability for space applications have not been thoroughly investigated, but reports to date suggest that they have excellent radiation tolerance [4].

II. EXPERIMENTAL

A. Photovoltaic Materials and Device Fabrication

Perovskite solar cells were fabricated on indium tin oxide (ITO) coated quartz substrates. We used quartz instead of using soda lime glass because the latter would become darkened by the radiation. The ITO had sheet resistance of $10 \Omega \text{ sq}^{-1}$. Prior to beginning cell fabrication, the ITO coated quartz substrates were cleaned with detergent, then ultrasonicated in acetone followed by 2-propanol.

In the fabrication process described below, the lead iodide was received from Alfa Aesar. Anhydrous N,N-dimethylformamide (DMF) and 2,2',7,7'-tetrakis (N,N-di-p-methoxyphenylamine)9,9'-spirobifluorene (spiro-OMeTAD) were received from Sigma Aldrich. Methylammonium iodide (MAI) and formamidinium iodide (FAI) were received from Dyesol.

The device architecture adopted in our study of electron irradiation is ITO/TiO₂/FAPbI₃/Spiro-OMeTAD/Ag. The TiO₂ compact layers were deposited on the ITO using electron-beam evaporation at a rate of 0.5 Å/s. The substrates were then transferred into a nitrogen-filled glove box and coated with the perovskite layer via a two-step spin-coating process. A precursor solution containing PbI₂ in DMF (600 mg ml⁻¹) was spin-coated first at 6000 rpm for 40 s and dried on a hotplate at 110 °C for 10 min. Then a FAI solution (70 mg ml⁻¹ in 2-propanol) was spin-coated onto the PbI₂ layer at 6000 rpm for 40 s, following by annealing on hotplate at 150 °C for 30 min. The hole transport layer was deposited by spin-

coating a 72 mg ml⁻¹ solution of spiro-OMeTAD solution in chlorobenzene, with additives of 18 μ l of lithium bis(trifluoromethanesulfonyl)imide (520 mg ml⁻¹ 1-butanol solution) and 29 μ l of 4-tert-butylpyridine per 1 ml of spiro-OMeTAD solution. Spin-coating was carried out in the glovebox at 2000rpm for 30s. Finally, a 100-nm silver electrode was thermally evaporated under vacuum ($\sim 10^{-7}$ Torr) at a rate of 1 $\text{\AA}/\text{s}$. A shadow mask was used to pattern the Ag such that each 1x1 cm quartz substrate contained (3) separate cells of 0.1 cm² nominal area.

A slightly different device architecture was adopted for our study of proton irradiation: ITO/NiO/ MAPbI₃/PCBM/Ag. The NiO layers were spin-cast from 0.1-molar nickel acetate and ethanolamine in ethanol solution and annealed at 300 $^{\circ}\text{C}$ for 1 hour. The substrates were then transferred into a nitrogen-filled glove box and coated with the perovskite layer via a one-step spin-coating process. A precursor solution containing 1-molar PbI₂ and MAI in DMF and DMSO (4:1 v/v) was spin-coated at 4000 rpm for 30 s, during which 100 μ l of chlorobenzene was dropped onto the spinning sample at the 10th second. Films were dried on a hotplate at 100 $^{\circ}\text{C}$ for 20 min. Then a solution of PCBM solution (20 mg ml⁻¹ in chlorobenzene) was spin-coated onto the MAPbI₃ layer at 1000 rpm for 60 s. The substrates, ITO, Ag, and cell form factor were otherwise the same as described above.

B. Electron and Proton Radiation Testing

We conducted electron irradiation testing with energy of 1 MeV at room temperature under vacuum of 10^{-5} Torr using a Dynamitron at NASA Jet Propulsion Laboratory. Fluence ranged from 10^{12} to 10^{16} cm⁻². The irradiation area was calibrated with a Faraday cup to be uniform (5%) within a 6 inch by 6 inch area to make sure each sample in the chamber receive the same dose. The cells' back contacts were placed to face the electron source to receive direct impacts of the electrons. This was necessary because of our use of relatively thick quartz superstrates, which would shield the cells from the electrons if irradiated from the front. Figure 1 shows the Monte Carlo simulation of the electron trajectories within the cells by using CASINO software package. Most of electrons penetrate the layers of solar cells with little scattering, and stop in the quartz substrate.

The proton irradiation tests were conducted with acceleration energy of 50 keV at the Aerospace Corporation. Fluence was set to 10^{12} cm⁻². The cells' back contacts were placed to face the proton source to receive direct impacts of the protons.

It is important to note that, because perovskite solar cells are known to degrade upon exposure to atmospheric moisture, it is possible that the cells' performance changed in the course of their transport to and from testing facilities, or during loading, unloading, and testing, which were performed in ambient air. To minimize this, cells were transported in partially evacuated desiccators, and stored either under

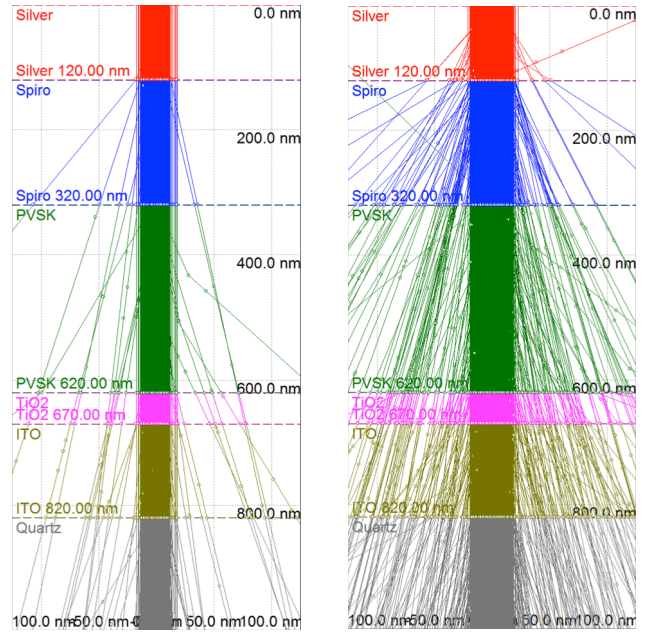


Figure 1. Simulation of 1-MeV electron trajectories with 10^{14} (left) and 10^{15} (right) fluences in the perovskite solar cells, showing most of electrons completely penetrate through all of the layers with little scattering. The electron beam radius is set to 17.845 nm.

vacuum or in nitrogen-purged dry boxes, such that total exposure to atmospheric air prior to final testing was typically on the order of several hours. Rather than testing each cell before and after irradiation, we instead prepared batches of control cells for each experiment. The control cells were fabricated and transported with the test cells, but instead of loading them into the vacuum chambers for irradiation, they were placed in a desiccator during this step. Both the test and the control cells were later characterized during the same measurement session.

C. Characterization

After the irradiation, the perovskite thin films and solar cells were removed from the vacuum chamber and transported to Caltech for characterization. Current density–voltage (J–V) characteristics of the photovoltaic cells were measured in ambient air using a Keithley 238 source meter unit under illumination at ~ 100 mW cm⁻² with a simulated AM 1.5G spectrum from an Oriel solar simulator (1 kW Xe arc lamp). The light intensity was calibrated using a hermetically sealed, 2x2 cm Si reference cell (PV Measurements, Inc) with calibration data from NREL. EQE measurements were carried out in ambient air using a Newport Xe arc lamp and monochromator.

III. RESULTS AND DISCUSSION

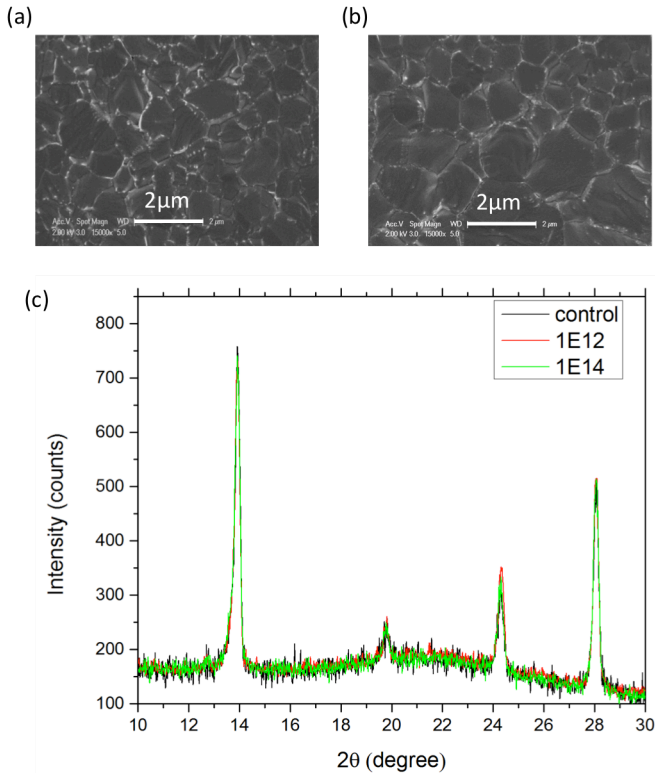


Figure 2. (a) SEM image of perovskite film without electron irradiation. (b) SEM image of perovskite film after 1 MeV electrons at fluence of 10^{14} cm^{-2} . (c) XRD patterns of perovskite films under different fluences of electron irradiation.

Figures 2(a) and (b) show the top-view scanning electron microscope (SEM) images of perovskite films without and with electron irradiation, respectively. The grain size of the perovskite film with electron irradiation is 0.5–2 μm , which is almost identical to that without irradiation. The same is true for their x-ray diffraction (XRD) patterns, as shown in Figure 2(c). The intense diffraction peak at $2\theta = 13.9^\circ$ represents highly oriented crystallinity with a strong preferred orientation of (110). No significant changes were observed from their morphology and crystal phase, which suggests the perovskite is physically resistant to the electron radiation.

Figure 3(a) shows the J–V curves of the perovskite solar cells with different electron radiation fluence. Control devices without electron irradiation exhibit a typical power conversion efficiency (PCE) of 12.2%, with a short-circuit current density (J_{SC}) of 21 mA cm^{-2} , an open-circuit voltage (V_{OC}) of 0.98 V, and a fill factor (FF) of 59%; which comparable with results of planar perovskite solar cells in the literature [5-8]. With electron fluence of 10^{12} , 10^{14} , and 10^{15} cm^{-2} , similar PCE values of 13.3%,

13.4%, and 12.4% were obtained, respectively. Figure 3(b) shows the external quantum efficiency (EQE), which is consistent with the measured J_{SC} in the devices. The spectral response did not change significantly with the fluence of electron radiation. Figure 3(c) summarizes the remaining factors of photovoltaic parameters of the perovskite solar cells with fluence up to 10^{16} cm^{-2} , where the FF and PCE still remain within 90% performance of the control cells. This degradation is substantially less than that reported for Si or III-V solar cells, and is within the range of sample-to-sample variability in our cells. Miyazawa et al. recently reported no detectable degradation of perovskite cell performance at this fluence and energy[4].

For proton testing, we carried out simulations of the irradiation to determine which layers of the cell structure would be affected, using SRIM/TRIM (Stopping and Range of Ions in Matter) software package. Figure 4(a) shows the particle trajectories for 30, 50, and 100 keV proton energy. In the 50-keV case, nearly all protons stop within the cell layers, with few reaching the quartz, but many reaching the ITO and NiO layers. Thus, this is a good energy to probe whether or not any cell layers are particularly sensitive to proton irradiation.

Figure 4(b) shows typical J–V curves of the perovskite solar cells before and after proton irradiation. The photovoltaic device before irradiation exhibits a typical PCE of 12.3%, with a J_{SC} of 17.7 mA cm^{-2} , a V_{OC} of 0.99 V, and a FF of 70%. After the proton irradiation, only the FF changed significantly, dropping to 42%, while the J_{SC} and V_{OC} remained largely unchanged. The apparent series resistance increased dramatically, from 3.8 to 24.5 Ωcm^{-2} . We note at this point the cells were tested under ambient air. We then loaded the cells into a vacuum chamber ($<10^{-6}$ Torr) and annealed them at 90 $^\circ\text{C}$ for 3 days. After cooling down to room temperature, we

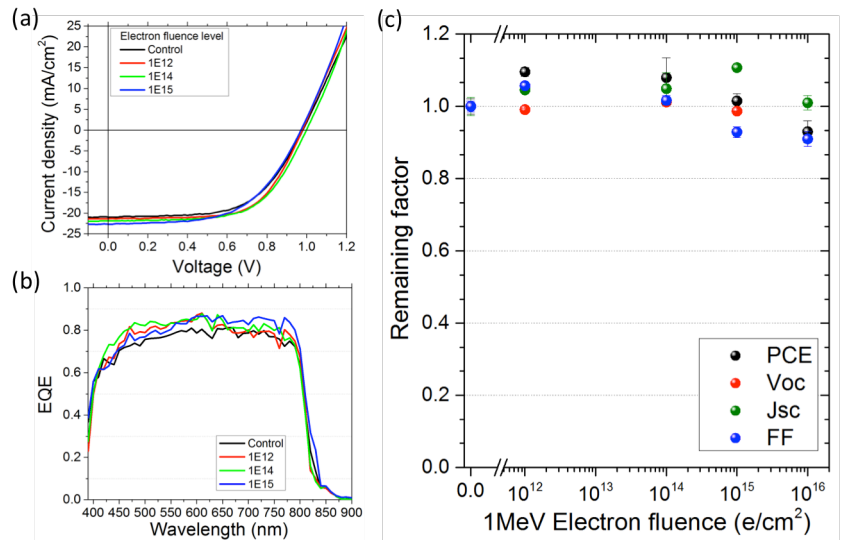


Figure 3. (a) J–V curves of the perovskite solar cells with different electron irradiation doses under one sun illumination. (b) Spectrum responses of these solar cells. (c) Remaining factors of photovoltaic parameters of the perovskite solar cells.

left the cells in the vacuum chamber and tested them under the solar simulator. (The vacuum chamber featured a quartz window and electrical feedthrough to facilitate J–V testing under vacuum.) Surprisingly, the cell performance recovered completely, with a PCE of 12.5% and FF of 67%. We hypothesize that (1) the implanted protons were removed from the cells during the vacuum annealing, and (2) the cations and anions in perovskites were able to migrate to their original locations in the crystal structure under the vacuum annealing. Further investigations are underway to understand the mechanism of damage recovery in perovskite solar cells.

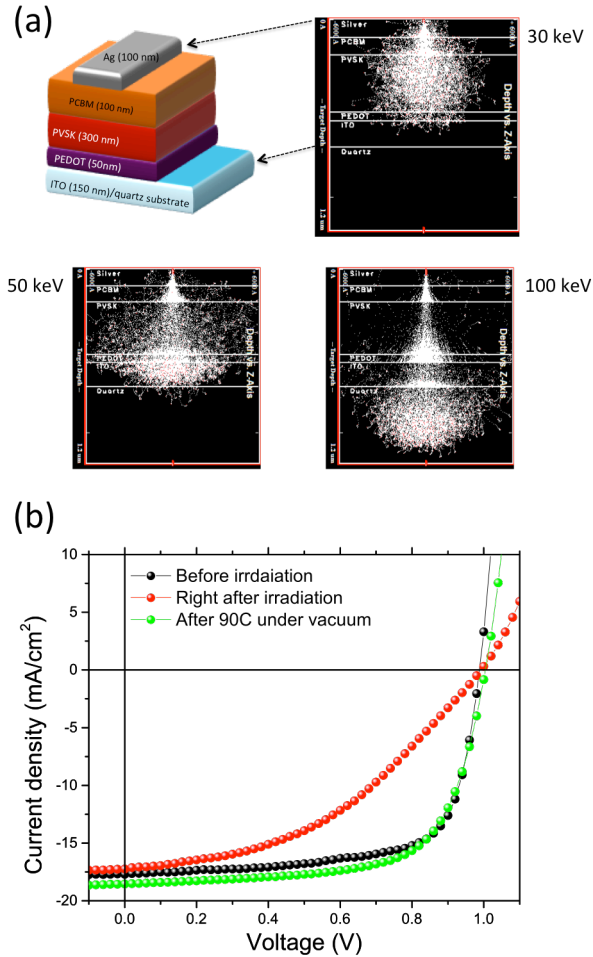


Figure 4. (a) Simulation of proton trajectories at energies from 30 to 100 keV in the perovskite solar cells. (b) J–V curves of the perovskite solar cells with before and after proton irradiation, as well as the recovering after vacuum annealing process.

IV. CONCLUSION

We have shown that perovskite solar cells are remarkably tolerant of 1 MeV electron and 50 keV proton radiation at fluence of up to 10^{16} and 10^{12} cm^{-2} , respectively. Electron

irradiation produced no detectable degradation at fluence up to 10^{15} cm^{-2} , and only caused $\sim 10\%$ degradation at 10^{16} cm^{-2} . This exceeds the reported performance of GaAs cells ($\sim 40\%$ degradation) and even radiation-hardened InP cells ($\sim 20\%$ degradation) at this fluence. [9,10] We further observed no significant changes to the morphology or crystal phase of the perovskite thin films under electron fluence of 10^{14} cm^{-2} .

Proton irradiation initially reduced the cells' efficiency by $\sim 40\%$, but interestingly, did not significantly impact V_{OC} or J_{SC} . This suggests that neither the cell's radiative efficiency nor its optical properties were damaged by the protons, and indeed, we found that a vacuum annealing process at 90 C completely restored the cell performance. We hypothesize that the cells should tolerate gradual exposure to proton irradiation at this energy, at operating temperatures typical for space solar cells, without requiring an explicit higher temperature annealing step.

The results suggest that perovskites have intrinsically superior radiation tolerance vs. established III–V space solar technologies. Thus, not only can perovskite solar cells offer higher specific power at the cell level, but they might require dramatically less (if any) radiation shielding to operate reliably in space.

ACKNOWLEDGEMENT

This work was funded by Northrop Grumman Corporation in the frame of Space Solar Power Initiative. The authors would like to thank Dennis Thorbourn at JPL for assisting operating Dynamitron.

REFERENCES

- [1] M. Yamaguchi, S. J. Taylor, S. Matsuda, O. Kawasaki, "Mechanism for the anomalous degradation of Si solar cells induced by high fluence 1 MeV electron irradiation", *Applied Physics Letters* **68**, 1996, pp. 3141–3143.
- [2] M. Kaltenbrunner, G. Adam, E. D. Glowacki, M. Drack, R. Schwodiauer, L. Leonat, D. H. Apaydin, H. Groiss, M. C. Scharber, M. S. White, N. S. Sariciftci, S. Bauer, "Flexible high power-per-weight perovskite solar cells with chromium oxide-metal contacts for improved stability in air", *Nat Mater* **14**, 2015, pp. 1032–1039.
- [3] "Alta Devices third generation (Gen3) product," 2016.
- [4] Y. Miyazawa, M. Ikegami, T. Miyasaka, T. Ohshima, M. Imaizumi, K. Hirose, "Evaluation of radiation tolerance of perovskite solar cell for use in space," in *Photovoltaic Specialist Conference (PVSC), 2015 IEEE 42nd*, New Orleans, LA, USA, 2015, pp. 1–4.
- [5] G. E. Eperon, V. M. Burlakov, P. Docampo, A. Goriely, H. J. Snaith, "Morphological Control for

- High Performance, Solution-Processed Planar Heterojunction Perovskite Solar Cells", *Advanced Functional Materials* **24**, 2014, pp. 151-157.
- [6] Q. Chen, H. P. Zhou, Z. R. Hong, S. Luo, H. S. Duan, H. H. Wang, Y. S. Liu, G. Li, Y. Yang, "Planar Heterojunction Perovskite Solar Cells via Vapor-Assisted Solution Process", *Journal of the American Chemical Society* **136**, 2014, pp. 622-625.
- [7] P.-W. Liang, C.-Y. Liao, C.-C. Chueh, F. Zuo, S. T. Williams, X.-K. Xin, J. Lin, A. K. Y. Jen, "Additive Enhanced Crystallization of Solution-Processed Perovskite for Highly Efficient Planar-Heterojunction Solar Cells", *Advanced Materials* **26**, 2014, pp. 3748-3754.
- [8] Y. Wu, A. Islam, X. Yang, C. Qin, J. Liu, K. Zhang, W. Peng, L. Han, "Retarding the crystallization of PbI₂ for highly reproducible planar-structured perovskite solar cells via sequential deposition", *Energy & Environmental Science* **7**, 2014, pp. 2934-2938.
- [9] M. Yamaguchi, "Radiation-resistant solar cells for space use", *Sol Energ Mat Sol C* **68**, 2001, pp. 31-53.
- [10] I. Weinberg, Radiation and temperature effects in gallium arsenide, indium phosphide, and silicon solar cells, National Aeronautics and Space Administration, [Washington, D.C.], 1987.